Available online at www.sciencedirect.com
ScienceDirect
Tetrahedron: Asymmetry
Tetrahedron: *Asymmetry* 19 (2008) 779–787

A theoretical investigation of the enantioselective reduction of prochiral ketones promoted by chiral diamines

Ling Sun, Mingsheng Tang,* Hongming Wang,* Donghui Wei and Lili Liu

Department of Chemistry, Center of Computational Chemistry, Zhengzhou University, Zhengzhou, Henan 450052, China

Received 29 October 2007; revised 2 December 2007; accepted 20 February 2008
Available online 15 April 2008

Abstract—A chiral diamide [(2*S*)-5-oxo-2-(arylamino)carbonylpyrrolidine] has been experimentally employed as an effective chiral catalytic precursor in the borane-mediated asymmetric reduction of prochiral ketones to produce the corresponding secondary alcohols. The mechanism of the reduction has been investigated theoretically by density functional theory, and the results reveal that this reaction is accomplished via four steps. Fully geometry optimized reactants, products, transition states, and intermediates are obtained. The analysis of these results reveals one pathway that is more energetically favorable, and its associated geometries correlate well with the final products of the reaction. Further calculations show that the solvent effect of toluene has no influence on the enantioselectivity of this reduction.

1. Introduction

With the presence of chiral catalysts,[1] numerous methodologies for the asymmetric reduction of ketones have been developed in the past decades, based on chiral or achiral reducing reagents. As more and more attention is paid in seeking ideal catalysts for the borane-mediated asymmetric reduction of prochiral ketones to obtain pure secondary alcohols, the development of chiral reducing catalysts has been, and continues to be, an area of interest in organic chemistry. This is due to the challenges involved in such endeavors as well as the applications of homochiral secondary alcohols in organic and medicinal chemistry.[2–8] There has already been much effort in designing and developing various types of chiral catalysts both experimentally and theoretically. For example, Corey et al.[7,9] originally utilized oxazaborolidines as chiral catalysts for the borane-mediated asymmetric reduction of prochiral ketones. There has also been extensive activity in studying chiral catalysts based on oxazaborolidine, titanium,[10,11] sulfonamide,[12,13] phosphorus,[14–16] and guanidine[8] derivatives to elucidate their high enantioselectivity. Recently, Basavaiah et al. reported[17] an experimental methodology employing the chiral diamine,[18] (2*S*)-2-anilinomethylpyrrolidine **1** (Fig. 1), as an efficient chiral catalytic source for the borane-mediated asymmetric reduction of prochiral ketones.[8,19–23] They also suggested a chiral diamine, (2*S*)-5-oxo-2-(arylamino) carbonylpyrrolidine **2** (Fig. 1), as a possible catalytic source for the same reduction.[24]

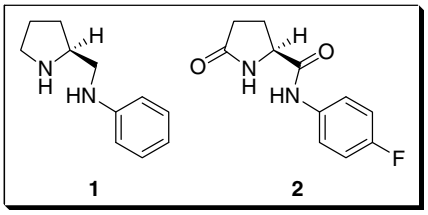

Figure 1. Structures of **1** and **2**.

There have been many theoretical reports investigating the reduction of ketones appearing in the literature. For example, theoretical investigation[1] of the oxazaborolidine-catalyzed reduction of ketones with BH_3 has been carried out and successfully explained the excellent enantioselectivity of the reaction. Tian and Li studied some of the key species of the catalytic cycle of pinacolone reduction[25,26] by means of HF/6-31G* calculations. Moreover, the mechanical study of stereoselectivity in the oxazaborolidine-catalyzed reduction of acetophenone has been carried[27] out using a variety of methods (AM1, HF, and DFT). The mechanism for the reduction of ketones to the corresponding alcohols, promoted by supercritical 2-propanol, was investigated.[28]

* Corresponding authors. E-mail addresses: hmwang06@163.com; mstang@zzu.edu.cn

0957-4166/$ - see front matter © 2008 Elsevier Ltd. All rights reserved.
doi:10.1016/j.tetasy.2008.02.020

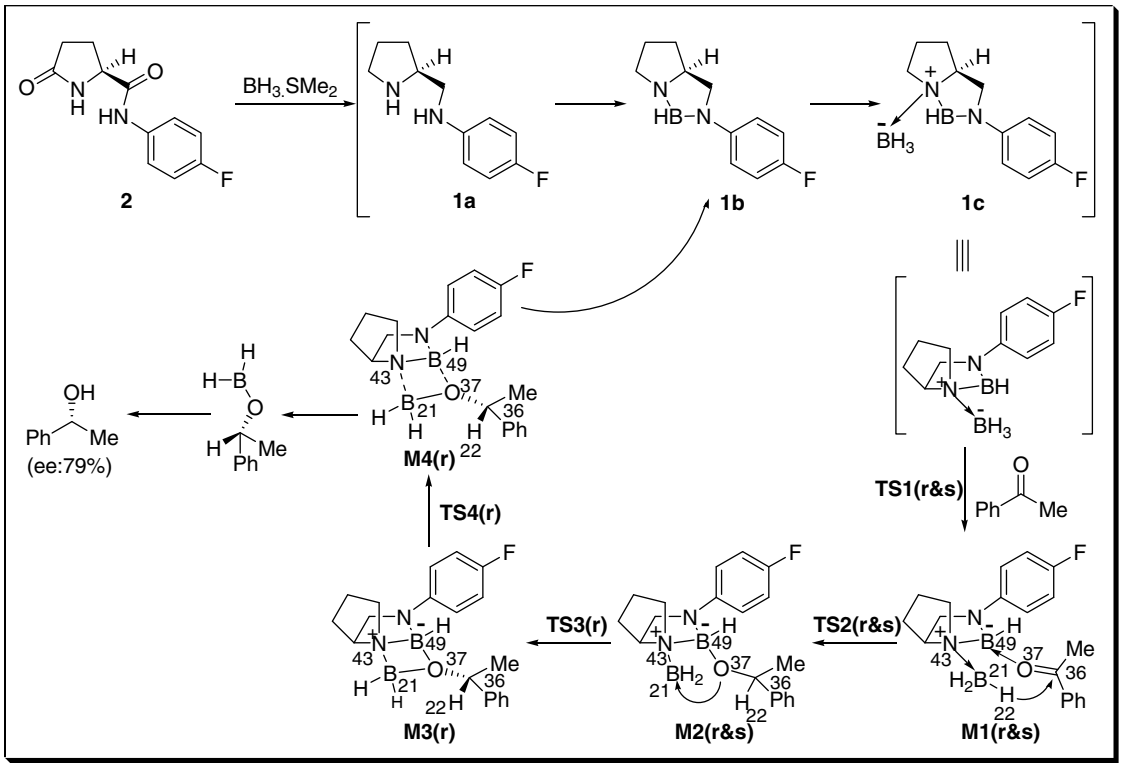

Scheme 1. The whole reaction mechanism.

Herein, we have undertaken electronic structure calculations in order to investigate the mechanism for this reaction and to interpret its stereoselectivity. Compound **2** was chosen as a representative of the possible catalysts capable of reducing the carbonyl substrate. Acetophenone is selected as the substrate for the borane-mediated asymmetric reduction. We believe that the reaction utilizes the following mechanism (Scheme 1).

All compounds shown in Scheme 1 will be referred to by their associated number in the interest of brevity. Initially **2** is reduced to **1a** by BH_3SMe_2, and then **1a** is converted successively into **1b** and **1c** (as can be seen in Scheme 1, **1b** is the true catalyst). The following processes, starting with the reaction between **1c** and acetophenone, are the focus of our investigation. The corresponding representation of the energy profile is illustrated in Figure 2.

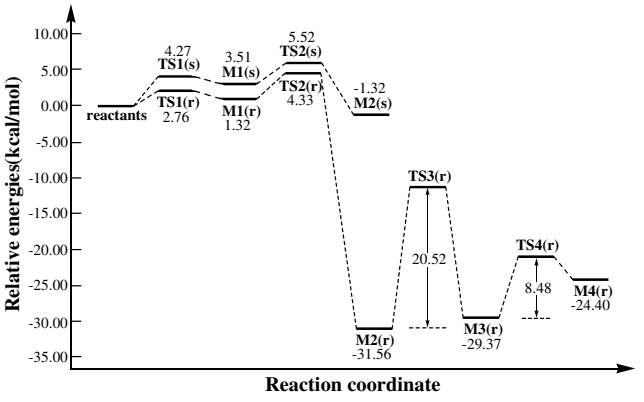

Figure 2. Potential energy profiles for the whole reaction along the reaction.

2. Computational details

All theoretical calculations were performed using the GAUSSIAN03[29] suite of programs. All structures were optimized by employing the hybrid density functional B3LYP method[30,31] and 6-31G(d,p) basis set. A vibrational frequency calculation was then performed at the optimized geometry belonging to each reactant, product, transition state, and intermediate. We confirmed that all reactants and intermediates have no imaginary frequencies, and each transition state has one, and only one, imaginary frequency. The zero-point energies (ZPE) were calculated using the vibrational frequencies. The intrinsic reaction coordinate (IRC) calculations, at the same level of theory, were performed to ensure that the transition states led to the expected reactants and products.

3. Results and discussion

We began by studying the chemical combination of **1c** with the acetophenone. Compound **1c** can initiate the reaction through two different positions because acetophenone has two very different functional groups attached to the carbonyl. The presence of two reaction sites gives rise to two distinct channels, resulting in two different diastereotopic

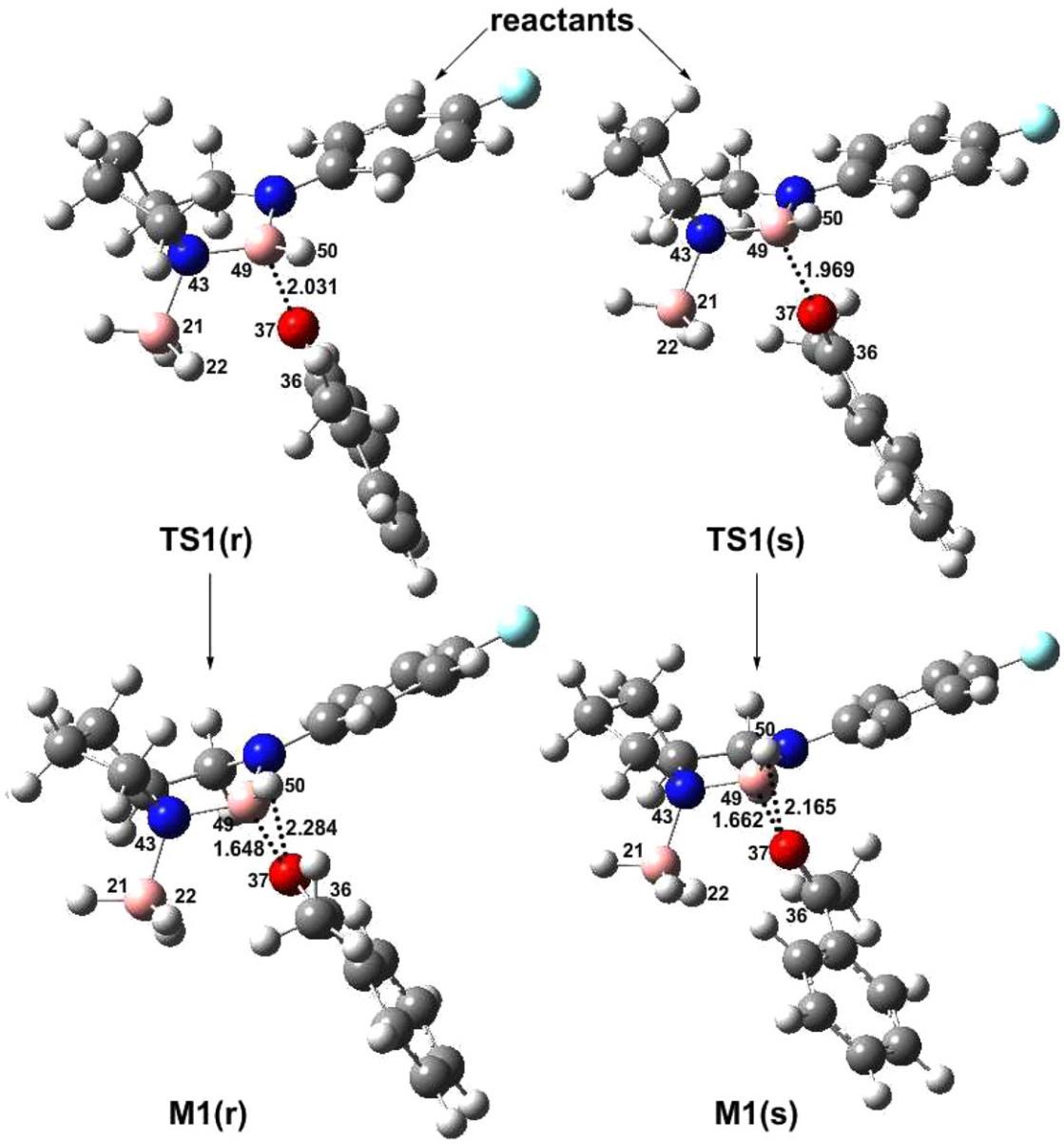

Figure 3. Representation of the optimized structures of the critical points **TS1**(**r**), **TS1**(**s**), **M1**(**r**), and **M1**(**s**) (units in Å for bond lengths).

transition states: **TS1**(**r**) and **TS1**(**s**) (Fig. 3). **TS1**(**r**) results from the approach of **1c** to the *Re* face of the ketone and leads to complex **M1**(**r**) (Fig. 3). In **TS1**(**r**), the B49–O37 bond is 2.031 Å and the energy of **TS1**(**r**) is calculated to lie 2.76 kcal/mol above that of the reactants. **TS1**(**s**) results from the approach of **1c** to the *Si* face of the ketone, and lies 4.27 kcal/mol above the energy of the reactants and leads to the other configuration **M1**(**s**) (Fig. 3). In **TS1**(**s**), the B49–O37 bond length is 1.969 Å.

The lower energy of **TS1**(**r**) compared to **TS1**(**s**) is most likely due to the difference of the steric interactions between the ketone substituents and the catalyst. **M1**(**r**) and **M1**(**s**) lie 1.32 and 3.51 kcal/mol above the energy of the reactants, respectively. The interaction of the electron-deficient boron atom, B49, and the lone pair on O37 of the ketone stabilizes the resulting complexes [the B49–O37 distance is 1.648 Å in **M1**(**r**) and 1.662 Å in **M1**(**s**)]. Furthermore, the hydrogen bonds [the distances between O37 and H50 are 2.284 Å and 2.165 Å in **M1**(**r**) and **M1**(**s**), respectively] formed between the carbonyl and H50 of the catalyst may lead to decreases in the energy barriers.

The second step is the transfer of H22 from the boron atom, B21, to the prochiral carbon atom, C36. The highly polarized carbonyl group exhibits strong chemical reactivity, hence the carbon atom C36 is easily attacked by nucleophilic reagents.

In both **M1**(**r**) and **M1**(**s**), the boron atom, B49, adopts a trigonal configuration and acts as a Lewis acid, which interacts with the O37 atom of the ketone. This kind of interaction leads to a great increase in the positive charge on the C36 atom belonging to the carbonyl group. Hence,

the attack on the C36 atom by a nucleophilic reagent at this site is increased. One possible source of nucleophilic atoms is B21, which has three nucleophilic hydrogen atoms. Furthermore, the O37 atom exerts an influence upon the nearby H22 atom, one of the three hydrogen atoms of the B21 atom, making it more nucleophilic. As a result of the above reasons, the H22 atom becomes the most nucleophilic among the three hydrogen atoms on B21 and is most easily transferred from the B21 atom to the electrophilic C36 atom. The transfer of the H22 atom in both **M1**(**r**) and **M1**(**s**), corresponding to the hydride atom attacking the *Re* face and *Si* face of the ketone, produces two diastereotopic transition states **TS2**(**r**) and **TS2**(**s**), respectively (Fig. 4).

In **TS2**(**r**), the distance between C36 and H22 is 1.769 Å, while the breaking B21–H22 bond is 1.264 Å. The B49–O37 bond is shortened from 1.648 Å in the structure of **M1**(**r**) to 1.556 Å in **TS2**(**r**). The energy of **TS2**(**r**) is higher than that of the reactants by 4.33 kcal/mol, and **TS2**(**r**) leads to intermediate **M2**(**r**), which has an (*R*)-configuration at the stereogenic center, C36.**TS2**(**s**) leads to the (*S*)-configuration, **M2**(**s**), and the newly forming C36–H22 bond is 1.812 Å, while the breaking B21–H22 bond is 1.259 Å. The energy of transition state **TS2**(**s**) is 5.52 kcal/mol above the energy of the reactants. Similar to **M1**(**r**) and **TS2**(**r**), the B49–O37 bond is shortened from 1.662 Å in **M1**(**s**) to 1.555 Å in **TS2**(**s**). The similarity in the energy of these two transition states can be mainly attributed to the similar stabilizing B49–O37 interaction [this distance is 1.556 Å in **TS2**(**r**) and 1.555 Å in **TS2**(**s**)]. The tiny difference in energy between **TS2**(**r**) and **TS2**(**s**) may be due to the different amounts of repulsion between the ketone substituent closest to the catalyst and the functional groups on the catalyst. The repulsion is much weaker in **TS2**(**r**) than that in **TS2**(**s**), because the distance between the closest ketone substituent and the catalyst in the former case is greater, according to the spatial structures of both transition states.

The free-energy difference between **TS2**(**r**) and **TS2**(**s**) is 1.78 kcal/mol. This value would correspond to an enantiomeric excess of about 83%, and thus does not exactly predict the experimental outcome (in comparison to an enantiomeric excess of about 79%). However, it does provide a correct indication of the stereochemical preference of the reaction, in agreement with the experimental evidence.[32]

The two diastereomeric reduced complexes, **M2**(**r**) and **M2**(**s**) (Fig. 5), are found 31.56 and 1.32 kcal/mol below the energy of the reactants, respectively, indicating that the hydride transfer from B21 to C36 is exothermic. The significantly lower energy of **M2**(**r**), relative to the energy of **M2**(**s**), also indicates that it should be the major product, and that this still will be crucial to determining the stereochemical outcome of the reaction. Ref. 32 shows that the hydride transfer step is clearly irreversible,[32] so the formation of the stereoisomer with an (*R*)-configuration at C36 is highly favored.

After the hydride transfer, the five-membered ring containing both N atoms opens by breaking the N43–B49 bond. The distance between the N43 atom and the B49 atom reaches its maximum at intermediates **M2**(**r**) and **M2**(**s**) (3.652 Å in **M2**(**r**) and 1.729 Å in **M2**(**s**)). This structural reconfiguration leads to a greater decrease of energy in **M2**(**r**) than it does in **M2**(**s**). At the same time, the bond lengths of the B49–O37 bond and the N43–B21 bond in **M2**(**r**) are shortened to 1.367 Å and 1.389 Å, respectively. Both bonds are shorter compared to 1.447 Å and 1.514 Å, respectively, in **M2**(**s**), causing greater stabilization of **M2**(**r**). Furthermore, the interaction between B49 and O37 makes the C36 atom more electrophilic in **M2**(**r**)

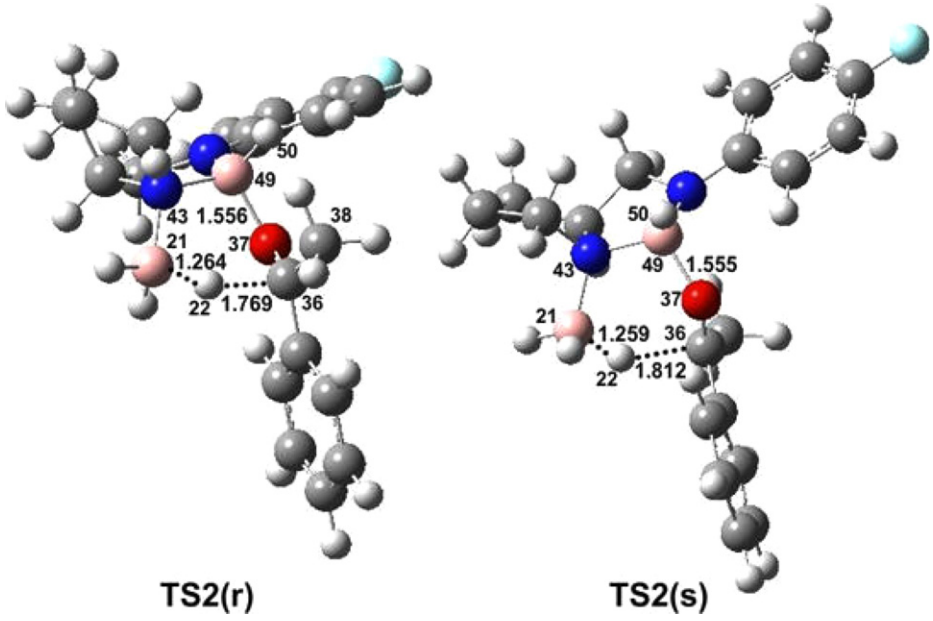

Figure 4. Optimized structures for **TS2**(**r**) and **TS2**(**s**) (units in Å for bond lengths).

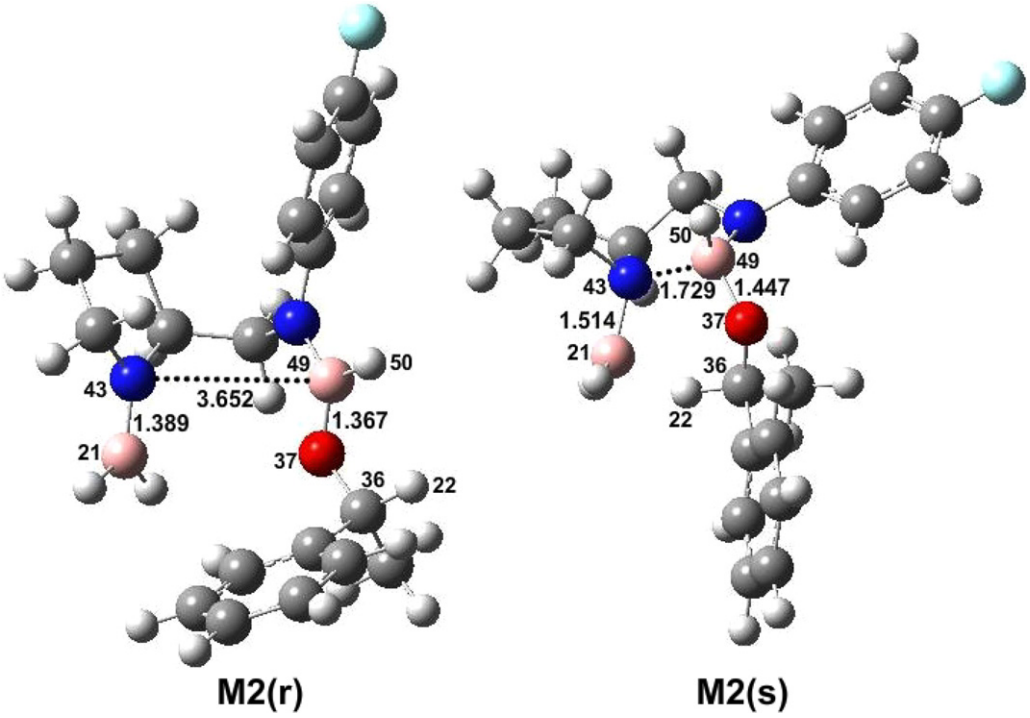

Figure 5. Representation of the optimized structures of the critical points **M2(r)** and **M2(s)** (units in Å for bond lengths).

Table 1. Some geometrical parameters and relative energies[a] of some stationary points along the reaction channels (units in Å for bond lengths, ° for bond angles)

R[b]				*S*[c]			
SP[d]	B49–O37	B49O37C36	RE[e]	SP	B49–O37	B49O37C36	RE
TS1(r)	2.031	134.9	2.76	**TS1(s)**	1.969	138.3	4.27
M1(r)	1.648	132.4	1.32	**M1(s)**	1.662	137.4	3.51
TS2(r)	1.556	123.9	4.33	**TS2(s)**	1.555	128.1	5.52
M2(r)	1.367	120.6	−31.56	**M2(s)**	1.447	123.1	−1.32

[a] Values are energies relative to reactants and are given in kilocalories per mole.
[b,c] The channels that **1c** approaches to the ketone from the *Re* face and *Si* face of the ketone, respectively.
[d] Stationary points.
[e] Relative energies.

than that in **M2(s)**, thereby making the interaction between C36 and H22 stronger in **M2(r)** than that in **M2(s)**. Thus, the B49–O37–C36 angles in all structures above are measured (Table 1).

According to Table 1, the B49–O37–C36 angles become smaller and smaller as the B49–O37 bonds become shorter and shorter in both channels, that is, the carbonyl group of the ketone can get closer to B49 and thus increases the stabilizing acid–base interaction, by decreasing the B49–O37–C36 angle which changes from roughly 180° of attack to 120.6° in **M2(r)** and 123.1° in **M2(s)**, to minimize the repulsive steric interactions of its substituent with the catalyst.

According to the above analysis, **M2(r)** is considered as the most likely reaction product, consistent with the experimental [the stereoisomer with an (*R*)-configuration at C36 is produced in 79% ee[24]]. Furthermore, the hydride transfer represents the rate-determining step for determining the stereochemical outcome of the reaction and is also clearly irreversible. Thus, we will focus on the **M2(r)** channel, which involves two processes: (1) the closure of the opened five-membered ring of the catalyst [corresponding to the **M2(r)**–**TS3(r)**–**M3(r)** transformation] (Fig. 6); and (2) the release of the oxaborane [corresponding to the **M3(r)**–**TS4(r)**–**M4(r)** transformation] (Fig. 7).

In process 1, the opened five-membered ring in the catalyst is closed, and a four-membered ring is formed through the [2+2] cycloaddition. The barrier for ring formation is 20.52 kcal/mol, and is mainly caused by the N43–B21 bond and the B49–O37 bond lengthening [the bond lengths of the N43–B21 and B49–O37 bonds increase to 1.483 Å and 1.453 Å, respectively, in **TS3(r)**] (Table 2).

The lengthening of the N43–B21 and B49–O37 bonds is due to the change in coordination of the B49 (from tri-coordinated to tetra-coordinated). In **TS3(r)**, the distance

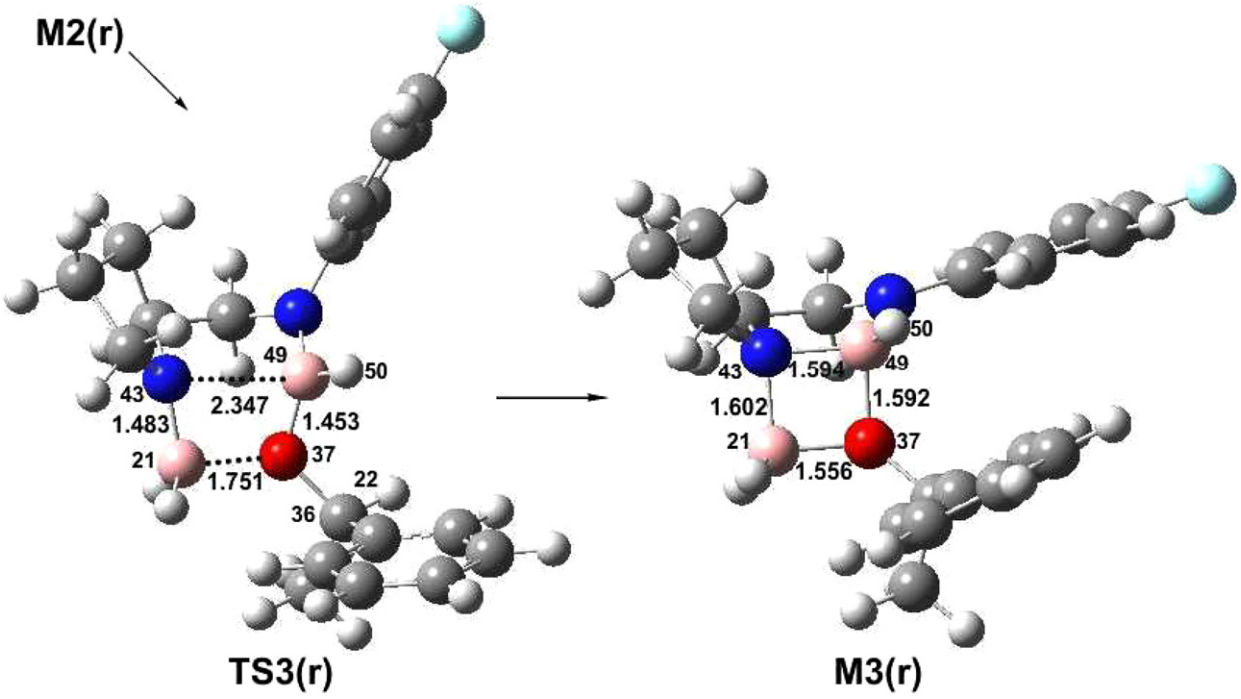

Figure 6. Optimized geometries of **TS3**(**r**) and **M3**(**r**) (units in Å for bond lengths).

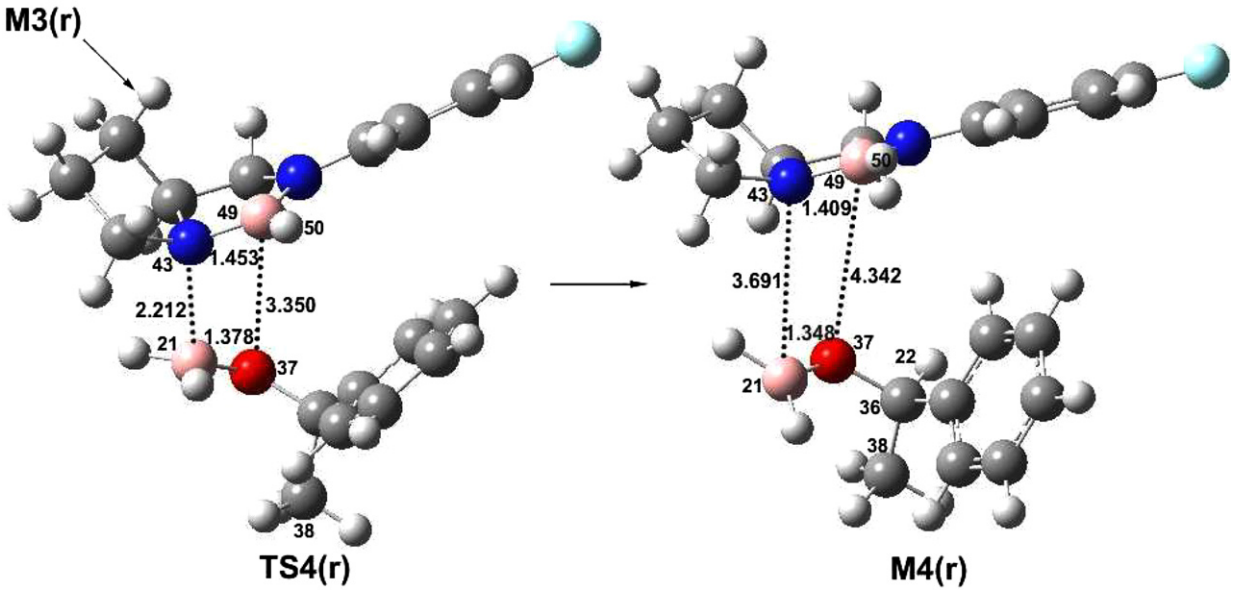

Figure 7. Optimized geometries of **TS4**(**r**) and **M4**(**r**) (units in Å for bond lengths).

between B49 and N43 is 2.346 Å, while the distance between O37 and B21 is 1.751 Å. This difference in bond lengths indicates that the B49–N43 and O37–B21 bonds are formed asymmetrically. In **M3**(**r**), the B49–N43 bond and the O37–B21 bond are 1.594 Å and 1.556 Å, respectively. The energy of **M3**(**r**) is 29.37 kcal/mol lower than that of the reactants and 2.20 kcal/mol higher than that of **M2**(**r**), which is mainly due to the strain in the newly formed four-membered ring. Additionally, the stabilizing B49–O37 and the N43–B21 interactions in **M3**(**r**) are weaker than those in **M2**(**r**) [the B49–O37 and N43–B21 distances are 1.592 Å and 1.602 Å in **M3**(**r**) and 1.389 Å and 1.367 Å in **M2**(**r**), respectively].

In process 2, oxaborane is released by breaking the N43–B21 and the B49–O37 bonds. This process occurs through the transition state **TS4**(**r**), leading to complex **M4**(**r**) whose barrier is 8.48 kcal/mol. In **TS4**(**r**), the B49–O37 and N43–B21 bonds lengthen to 3.350 Å and 2.212 Å, while the B49–N43 and the O37–B21 bonds contract to 1.453 Å and 1.378 Å, respectively (Table 2). **M4**(**r**) is now composed of two segments, catalyst **1b** and the oxaborane that can

Table 2. Some geometrical parameters and relative energies[a] of **M2**(**r**), **TS3**(**r**), **M3**(**r**), **TS4**(**r**), and **M4**(**r**) (units in Å for bond lengths)

SP[b]	B49···O37	N43···B21	B49···N43	O37···B21	RE[c]
M2(**r**)	1.367	1.389	3.652	—	−31.56
TS3(**r**)	1.453	1.483	2.346	1.751	−11.04
M3(**r**)	1.592	1.602	1.594	1.556	−29.37
TS4(**r**)	3.35	2.212	1.453	1.378	−20.89
M4(**r**)	4.342	3.691	1.409	1.348	−24.4

[a] Values are energies relative to reactants and are given in kilocalories per mole.
[b] Stationary points.
[c] Relative energies.

be worked up to form a secondary alcohol. In fact, the two segments still interact slightly with each other, since the N43–B21 distance is 3.691 Å and the B49–O37 distance is 4.342 Å. In **M4**(**r**), the bond length of B49–N43 is 1.409 Å, nearly equal to the B49–N43 bond length in **1b**, implying that **M4**(**r**) is similar to the catalyst in its initial state. The O37–B21 bond decreases even more in going from **TS3**(**r**) to **M4**(**r**) with a final value of 1.348 Å. The energy of **M4**(**r**) is 24.40 kcal/mol, which is lower than the reactant's energy; therefore, the overall reaction is an exothermic process.

At last, the solvent effect of toluene on the enantioselectivity of this reduction has also been taken into account. We have re-computed the two transition states **TS2**(**r**) and **TS2**(**s**) and two intermediates **M2**(**r**) and **M2**(**s**) in toluene, using the PCM method by means of geometrical optimizations.

The results are **TS2′**(**r**), **TS2′**(**s**), **M2′**(**r**), and **M2′**(**s**), respectively, and are represented in Figures 8 and 9. **TS2′**(**r**) is the transition state leading to the intermediate with (*R*)-configuration at C36, **M2′**(**r**) is 1.20 kcal/mol more stable than **TS2′**(**s**) leading to the opposite configuration, **M2′**(**s**). The energy of **M2′**(**r**) is 29.29 kcal/mol lower than that of **M2′**(**s**). The results indicate that for the product an excess of the stereoisomer with (*R*)-configuration at C36 is again in agreement with the experimental outcome.

4. Conclusions

In this paper, a DFT investigation has been carried out to show an integrated mechanism for the catalytic reduction of prochiral ketones. The results reveal that this reduction takes place via four steps: initially **1c** approaches the carbonyl group of the ketone. The second step is a hydride transfer, which can occur via two different pathways, each having a diastereotopic transition state. One pathway corresponds to the attack of the hydride at the *Re* face while the other pathway involves an attack at the *Si* face. Our calculations indicate that the stereoisomer with an (*R*)-configuration at the new stereogenic center is significantly more energetically favorable. The energetic favorability of the (*R*)-configuration stereoisomer suggests that it will be the dominant product, which is in good agreement with experiment. The two remaining steps involve the closure of the five-membered ring of the catalyst and the release of the oxaborane. The former step occurs through a [2+2] cycloaddition to give rise to a new four-membered ring, while in the latter step the oxaborane is released by

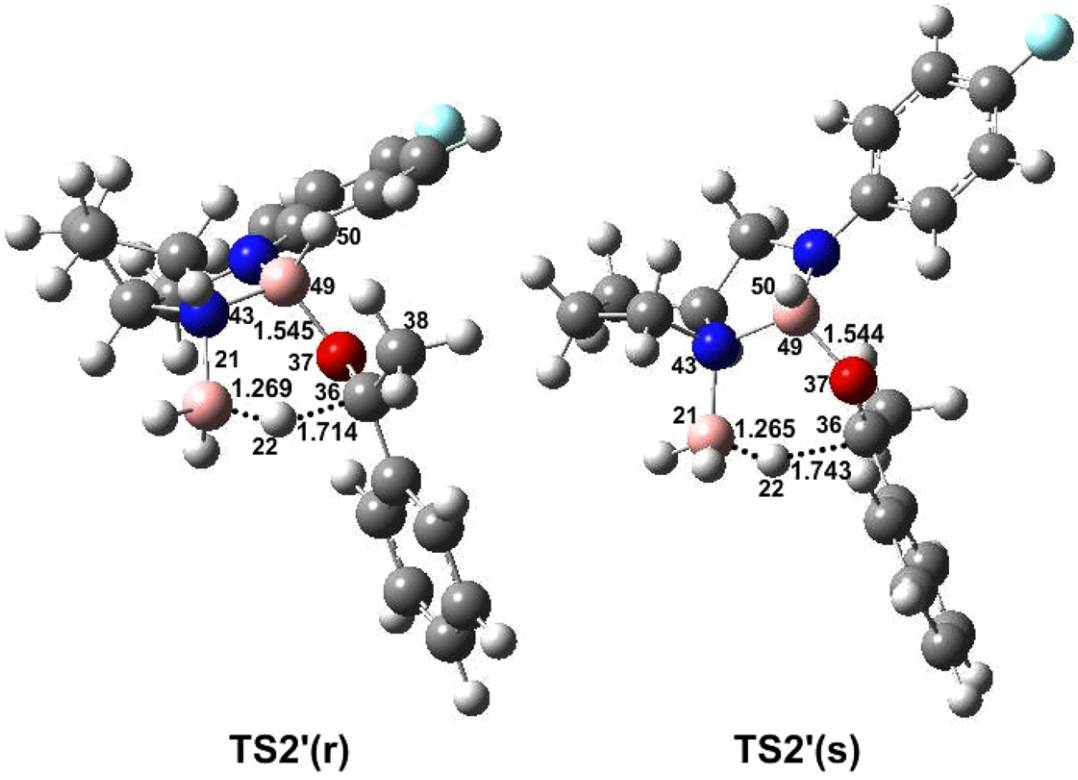

Figure 8. Optimized structures for **TS2′**(**r**) and **TS2′**(**s**) (units in Å for bond lengths).

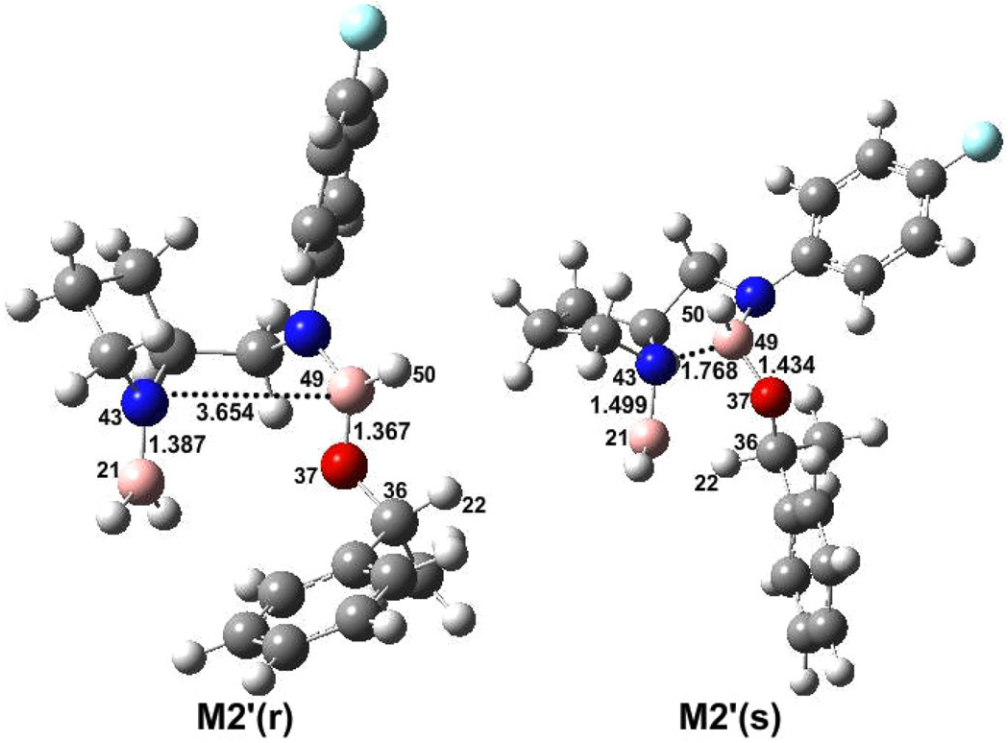

Figure 9. Optimized structures for **M2′(r)** and **M2′(s)** (units in Å for bond lengths).

breaking two bonds of the four-membered ring. The calculations also indicate that the solvent effect of toluene has not influenced the enantioselectivity of this reduction.

Acknowledgment

The work described in this paper was supported by the National Natural Science Foundation of China (No. 20672104).

References

1. Corey, E. J.; Helal, P. J. *Angew. Chem., Int. Ed.* **1998**, *37*, 1986–2012.
2. Brown, H. C.; Jadhav, P. K.; Singaram, B. *Mod. Synth. Methods* **1986**, *4*, 307–356.
3. Brown, H. C.; Ramachandran, P. V. *Acc. Chem. Res.* **1992**, *25*, 16–24.
4. Singh, V. K. *Synthesis* **1992**, *7*, 607–617.
5. Wallbaum, S.; Martens, J. *Tetrahedron: Asymmetry* **1992**, *3*, 1475–1504.
6. Deloux, L.; Srebnik, M. *Chem. Rev.* **1993**, *93*, 763–784.
7. Corey, E. J.; Helal, C. J. *Angew. Chem., Int. Ed.* **1998**, *37*, 1986–2012.
8. Basavaiah, D.; Venkateswara Rao, K.; Sekhara Reddy, B. *Tetrahedron: Asymmetry* **2006**, *17*, 1036–1040.
9. Corey, E.; Bakshi, R. K.; Shibata, S. *J. Am. Chem. Soc.* **1987**, *109*, 5551–5553.
10. Giffels, G.; Dreisbach, C.; Kragl, U.; Weigerding, M.; Waldmann, H.; Wandrey, C. *Angew. Chem., Int. Ed. Engl.* **1995**, *34*, 2005–2006.
11. Sarvary, I.; Almqvist, F.; Frejd, T. *Chem. Eur. J.* **2001**, *7*, 2158–2166.
12. Hu, J.-b.; Zhao, G.; Yang, G.-s.; Ding, Z.-d. *J. Org. Chem.* **2001**, *66*, 303–304.
13. Hu, J.-b.; Zhao, G.; Ding, Z.-d. *Angew. Chem., Int. Ed.* **2001**, *40*, 1109–1111.
14. Burns, B.; Studley, J. R.; Wills, M. *Tetrahedron Lett.* **1993**, *34*, 7105–7106.
15. Gamble, M. P.; Smith, A. R. C.; Wills, M. *J. Org. Chem.* **1998**, *63*, 6068–6071.
16. Buono, G.; Chiodi, O.; Wills, M. *Synlett* **1999**, *4*, 377–388.
17. Basavaiah, D.; Venkateswara Rao, K.; Sekhara Reddy, B. *Tetrahedron: Asymmetry* **2006**, *17*, 1041–1044.
18. (a) Asami, M.; Sato, S.; Watanabe, H. *Chem. Lett.* **2000**, *9*, 990–991; (b) Sato, S.; Watanabe, H.; Asami, M. *Tetrahedron: Asymmetry* **2000**, *11*, 4329–4340.
19. Basavaiah, D.; Chandrashekar, V.; Das, U.; Jayapal Reddy, G. *Tetrahedron: Asymmetry* **2005**, *16*, 3955–3962.
20. Basavaiah, D.; Jayapal Reddy, G.; Venkateswara Rao, K. *Tetrahedron: Asymmetry* **2004**, *15*, 1881–1888.
21. Basavaiah, D.; Jayapal Reddy, G.; Chandrashekar, V. *Tetrahedron: Asymmetry* **2004**, *15*, 47–52.
22. Basavaiah, D.; Jayapal Reddy, G.; Chandrashekar, V. *Tetrahedron: Asymmetry* **2002**, *13*, 1125–1128.
23. Basavaiah, D.; Jayapal Reddy, G.; Chandrashekar, V. *Tetrahedron: Asymmetry* **2001**, *12*, 685–689.
24. Basavaiah, D.; Venkateswara Rao, K.; Sekhara Reddy, B. *Tetrahedron: Asymmetry* **2007**, *18*, 968–974.
25. Li, M.; Tian, A. *THEOCHEM* **2001**, *544*, 37–47.
26. Li, M.; Tian, A. *THEOCHEM* **2001**, *544*, 25–35.
27. Alagona, G.; Ghio, C.; Persico, M.; Tomasi, S. *J. Am. Chem. Soc.* **2003**, *125*, 10027–10039.
28. Kamitanaka, T.; Matsuda, T.; Harada, T. *Tetrahedron* **2007**, *63*, 1429–1434.
29. Frisch, M. J.; Trucks, G. W.; Schlegel, H. B.; Scuseria, G. E.; Robb, M. A.; Cheeseman, J. R.; Montgomery, J. A.; Vreven,

T. Jr.; Kudin, K. N.; Burant, J. C.; Millam, J. M.; Iyengar, S. S.; Tomasi, J.; Barone, V.; Mennucci, B.; Cossi, M.; Scalmani, G.; Rega, N.; Petersson, G. A.; Nakatsuji, H.; Hada, M.; Ehara, M.; Toyota, K.; Fukuda, R.; Hasegawa, J.; Ishida, M.; Nakajima, T.; Honda, Y.; Kitao, O.; Nakai, H.; Klene, M.; Li, X.; Knox, J. E.; Hratchian, H. P.; Cross, J. B.; Bakken, V.; Adamo, C.; Jaramillo, J.; Gomperts, R.; Stratmann, R. E.; Yazyev, O.; Austin, A. J.; Cammi, R.; Pomelli, C.; Ochterski, J. W.; Ayala, P. Y.; Morokuma, K.; Voth, G. A.; Salvador, P.; Dannenberg, J. J.; Zakrzewski, V. G.; Dapprich, S.; Daniels, A. D.; Strain, M. C.; Farkas, O.; Malick, D. K.; Rabuck, A. D.; Raghavachari, K.; Foresman, J. B.; Ortiz, J. V.; Cui, Q.; Baboul, A. G.; Clifford, S.; Cioslowski, J.; Stefanov, B. B.; Liu, G.; Liashenko, A.; Piskorz, P.; Komaromi, I.; Martin, R. L.; Fox, D. J.; Keith, T.; Al-Laham, M. A.; Peng, C. Y.; Nanayakkara, A.; Challacombe, M.; Gill, P. M. W.; Johnson, B.; Chen, W.; Wong, M. W.; Gonzalez, C.; Pople, J. A. GAUSSIAN *03, Revision C.02*; Gaussian: Wallingford, CT, 2004 (SN: PC21390756W-4203N).

30. Becke, A. D. *J. Chem. Phys.* **1993**, *98*, 5648–5652.
31. Lee, C.; Yang, W.; Parr, R. G. *Phys. Rev. B* **1988**, *37*, 785–789.
32. Bandini, M.; Bottoni, A.; Cozzi, P. G.; Miscione, G. P.; Monari, M.; Pierciaccante, R.; Umani-Ronchi, A. *Eur. J. Org. Chem.* **2006**, *20*, 4596–4608.